ELSEVIER

Biophysical Chemistry 106 (2003) 253–265

Biophysical Chemistry

www.elsevier.com/locate/bpc

New pinch-porphyrin complexes with quantum mixed spin ground state $S=\frac{3}{2},\frac{5}{2}$ of iron (III) and their catalytic activity as peroxidase

Amparo Sánchez-Sandoval[a], Daniel Ramírez-Rosales[b], Rafael Zamorano-Ulloa[b], Cecilio Álvarez-Toledano[c], Mónica Moya-Cabrera[c], Yasmi Reyes-Ortega[a,*]

[a]*Centro de Química, Instituto de Ciencias, Universidad Autónoma de Puebla. 14 Sur 6301. Col. San Manuel, Puebla, Pue 72570, Mexico*

[b]*Escuela Superior de Física y Matemáticas, Instituto Politécnico Nacional. Ave. Instituto Politécnico Nacional S/N, Edif. 9, Unidad Profesional Adolfo López Mateos, San Pedro Zacatenco, Mexico D.F. 07738, Mexico*

[c]*Instituto de Química, Universidad Nacional Autónoma de México. Circuito exterior S/N, Ciudad Universitaria, Mexico D.F. 04510, Mexico*

Received 17 February 2003; received in revised form 6 June 2003; accepted 7 June 2003

Abstract

New complexes of the pinch-porphyrin family were obtained from the dimethylester of (*proto*-, *meso*-, and *deutero*-porphyrinato)iron(III) with the ligand [*N*,*N*′-bis-pyridin-2-ylmethyl-propane-1,3-diamine] **1**–**3** and with the ligand [*N*-pyridin-2-ylmethyl-*N*′-{3-[(pyridin-2-ylmethyl)-amino]-propyl}-propane-1,3-diamine] **4**–**6**. The UV/VIS studies of **1**–**6** indicate an increase in the distortion of the ligand field excited state. The ^{1}H NMR spectra of **1**–**6** at RT and over the range 223–328 K show iron(III)-complexes with quantum mixed spin state (qms) $S=\frac{5}{2}$, $S=\frac{3}{2}$. The chemical shifts of the *meso* protons are consistent with qms state $S=\frac{3}{2}$, $S=\frac{5}{2}$, where the $S=\frac{3}{2}$ spin state is lowest in energy. For methyl-heme the chemical shifts are also consistent with a qms state but now the $S=5/2$ ground state is lowest in energy. ESR spectra of **1**–**6** show two different species, B and C, of iron(III) with qms, $S=\frac{5}{2}$, $S=\frac{3}{2}$ consistent with the ^{1}H NMR results. Species B with 70% of $S=\frac{5}{2}$ and species C with 72.5% of $S=\frac{3}{2}$. The catalytic activity as peroxidase of **1**–**6** was quantified by guaiacol test; their theoretical maximum rate constants were $k_{cat}\sim 10^2$–10^3 $M^{-1}\,s^{-1}$. A quantitative empirical correlation is found: the higher the $\frac{3}{2}$ spin contribution to the qms state and the

*Corresponding author. Fax: +52-22-2955-51.

E-mail address: yreyes@siu.buap.mx (Y. Reyes-Ortega).

0301-4622/03/$ - see front matter
doi:10.1016/S0301-4622(03)00186-8

higher proportion of this species into the samples, the higher the peroxidase activity. Such a correlation was also obtained for pinch-porphyrins already reported.

Keywords: Peroxidase; Catalytic and kinetic models compounds; Quantum mixed spin state $S=\frac{5}{2}$, $S=\frac{3}{2}$ of iron(III)

1. Introduction

The magnetic states in iron porphyrins are the driving force for the diverse and versatile behavior of their chemistry. Spin state of iron ion is determined by the ligand field strength and the symmetry of the surrounding ligands [1–3]. In haem proteins, the magnetic state has long been recognized as a convenient indicator of chemical co-ordination as well as subtle biochemical properties [4]. In the biological compounds as ferricytochrome *c*′, horseradish peroxidase and the ferric ion in complexes of tetragonal symmetry, the ground state is composed of the linear combination of two spin states, $S=\frac{5}{2}$ and $S=\frac{3}{2}$ [4–6]. Other systems of iron(III) with qms also have been reported [7–14]. These systems have mostly five-co-ordinated iron in ligand fields produced by anions, producing a weak tetragonal field around iron(III) [1,13]. In accord to Nesset et al. [13], the qms $S=\frac{5}{2}$, $S=\frac{3}{2}$ of iron(III) complexes exhibit a wide range of physical properties such as magnetic moments between 4.0–5.8 μ_B at RT, curved Weiss–Curie plots and ESR effective $g_\perp$ values of 4.2–5.8 [12–18].

Reyes et al. [14] reported novel model compounds of peroxidases, pinch-porphyrins. In these two axial pyridine ligands bonded through a chain of nine atoms (pinch picdien ligand = *N*-pyridin-2-ylmethyl-*N*′-{2-[(pyridin-2-ylmethyl)-amino]-ethyl}-ethane-1,2-diamine) occupied the fifth and sixth position of iron–porphyrin, in consequence it was expected a low spin state for iron(III); nevertheless, they showed a qms for iron(III). The pinch ligand controls the co-ordination of the pyridine groups producing a weak tetragonal ligand field [13]. These pinch-porphyrins resulted in successful models of iron(III) qms systems and the best kinetic model of peroxidases is yet to be reported [14]. The pinch ligand significantly alters the iron environment in these complexes, producing physical characteristics of qms of the iron(III) which correlate with (a) displacement of iron(III) out of porphyrin plane, (b) contraction of porphyrin core, and (c) catalytic activity [13,14]. In this paper we report six new pinch-porphyrin–iron(III) complexes **1–6** (Fig. 1). The new pinch ligands, picpropylen and picdipropylen, are two atoms shorter and two atoms larger than the original pinch ligand (picdien), respectively [14]. The complexes were studied by UV/VIS, ^{1}H NMR, ESR spectroscopies and kinetically as peroxidases by guaiacol test [19]. Herein, we report the effect of the chain size of the pinch-axial ligands on the structure, the qms of iron(III), the ratio of the

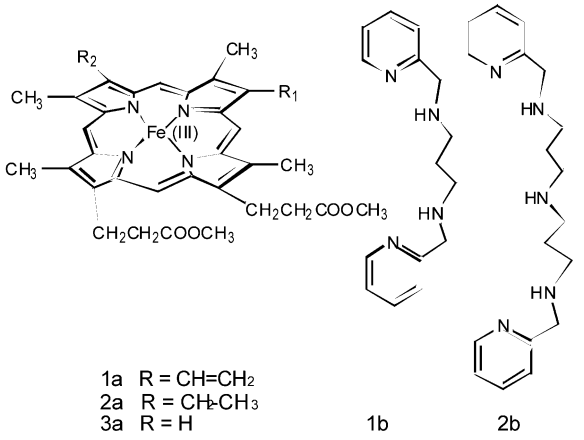

Fig. 1. (1a) [chloro-protoporphyrinato dimethyl ester]iron(III); (2a) [chloro-mesoporphyrinato dimethyl ester]iron(III); (3a) [chloro-deuteroporphyrinato dimethyl ester]iron(III); (1b) *N*,*N*′-bis-pyridin-2-ylmethyl-propane-1,3-diamine); (2b) (picpropylen); *N*-pyridin-2-ylmethyl-*N*′-{3-[(pyridin-2-ylmethyl)-amine]-propyl}-propane-1,3-diamine (picdipropylen).

mixtures of $S=\frac{3}{2}$, $S=\frac{5}{2}$ and its correlation to catalytic activity as peroxidase.

2. Experimental

2.1. Instruments

ESR spectra were recorded in methanolic solutions at ca. 1 mM. The microwave X-band (9.4 GHz) of a JEOL JES-RES3X spectrometer at 77 K was used. The *g* values were accurately determined by two methods. One used Mn(II) weak pitch standard and the other the precise reading of microwave frequency (± 1 KHz) and of the magnetic field (± 0.1 Gauss).

NMR measurements were carried out on a JEOL Eclipse 300 spectrometer at variable temperature (-55 to $+55$ °C), using methanolic sample solution at ca. 1 mM. These **1**–**6** complexes are stable in methanolic solution in this temperature range. At lower temperatures, water condensation at the exterior of the NMR tube wall greatly deteriorates the signal. Electronic spectra were recorded in a Shimadzu UV/VIS/NIR 3100 spectrophotometer on ca. 1–0.001 mM methanolic sample solution, at 300 K, using cells with 1 cm path length.

2.2. Materials

Spectrophotometric and kinetic measurements were made in anhydrous methanol. The iron–porphyrins were prepared as described previously [20]. Compounds *N*,*N*′-bis-pyridin-2-ylmethyl-propane-1,3-diamine (picpropylen) and *N*-pyridin-2-ylmethyl-*N*′-{3-[(pyridin-2-ylmethyl)-amine]-propyl}-propane-1,3-diamine (picdipropylen) were prepared by the Sánchez-Sandoval et al. method [21]. The kinetic experiments were made in aqueous 20.1 mM solutions of guaiacol; the porphyrin–iron methanolic solutions were 0.015–0.030 mM and the hydrogen peroxide solution was 1.3–1.6 M.

2.3. Preparation of pinch-porphyrin *1–6* complexes

All complexes were synthesized using the Reyes-Ortega et al. method [14]. Porphyrin–iron(III) complexes were dissolved in methanol and treated separately with picpropylen and picdipropylen in equimolecular quantities. The mixtures were stirred for 6 h. In another experiment the methanolic solutions of precursor porphyrins were titrated with picpropylen and picdipropylen solutions in methanol, separately, until reaching one equivalent. The spectroscopic results were the same in both routes. Spectroscopic and kinetic studies were directly performed on the reaction solutions.

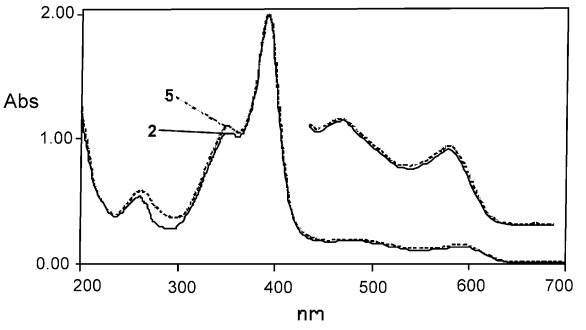

Fig. 2. The UV/VIS spectra of complexes [(picpropylen)(mesoporphyrinato dimethyl ester)]iron(III) **2** (——) and [(picdipropylen)(mesoporphyrinato dimethyl ester)]iron(III) **5** (----).

2.4. Kinetic studies

Rate determination of iron–porphyrin-catalyzed oxidation of guaiacol [19] with hydrogen peroxide was carried out as previously described for pinch-porphyrin-iron(III) [14].

3. Results and discussion

3.1. UV/VIS spectroscopy

The UV/VIS spectra of **2** and **5** are shown in Fig. 2. These spectra are representative of all the pinch-complexes. The spectra show an intense Soret band and two weak *Q* bands characteristic of porphyrin iron(III) systems in a $\leq D_{4h}$ symmetry [22–25]. The spectroscopy data are shown in Table 1. Compounds **2**, **3**, **5** and **6** show one intense shoulder at 342.0–351.0 nm. Shoulders of this kind have been reported for some native

Table 1
Optical absorption spectra of **1–6** complexes

Pinch-porphyrin	λ_{max} (MeOH)/nm			
	Shoulder	Soret	Band Q_1	Band Q_2
1		398.0	484.5	593.5
2	351.0	391.5	479.0	591.5
3	342.5	391.5	478.0	584.0
4		398.0	481.5	594.0
5	350.0	391.5	479.5	591.0
6	342.5	391.5	476.0	584.5

enzymes [3,4,26–30]. The *Q* bands of **1–6** are more intense than the *Q* bands of their corresponding precursors, pinch ligand-free porphyrins. This behavior indicates that the distortion into the ligand field excited state is higher in the presence of the pinch ligand [14,25].

3.2. Proton NMR spectroscopy

Table 2 shows the chemical shifts of ^{1}H NMR/CD_3OD spectra of **1–6** pinch-porphyrins at RT (Fig. 3). Assignment of the signals is based on

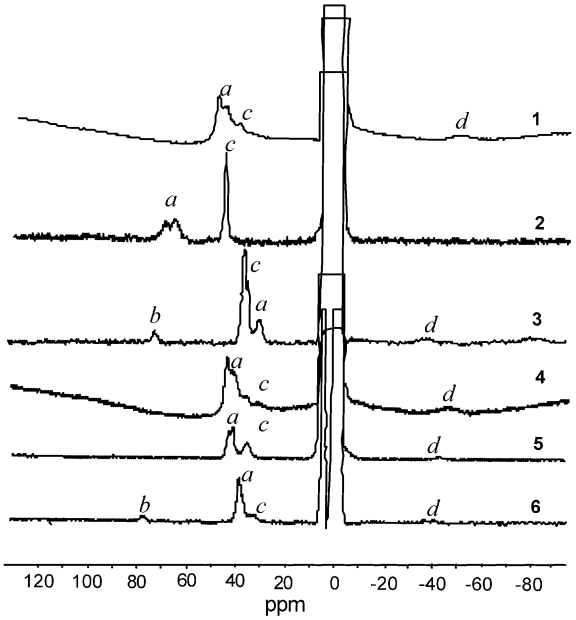

Fig. 3. The 300 MHz ^{1}H NMR spectra of **1–6** complexes. In all cases, the heme substituents are labeled (a) heme-CH_3; (b) 2,4-H; (c) α-CH_2; (d) meso-H [29–37].

Table 2
Proton NMR data[a] of **1–6** complexes

Pinch-porphyrin	$\delta_{heme\text{-}CH_3}$	Spread $\delta_{heme\text{-}CH_3}$	Average $\delta_{heme\text{-}CH_3}$	Q_{asym}	$\delta_{2\text{-}4\text{-}H}$	$\delta_{H\text{-}meso}$	$\delta_{\alpha\text{-}CH_2}$
1	40.12 38.35 37.50	2.62	38.65	0.067		−35.28	33.54
2	67.53 64.39	3.14	65.96	0.047			45.10
3	40.72 39.99 38.54	2.18	39.75	0.054	76.75	−32.27	34.13
4	40.19 38.20 36.14 33.47	6.72	37.00	0.181		−35.36	29.47
5	40.15 39.11 34.02	6.13	37.76	0.16		−35.0	34.06
6	40.16 34.76	5.4	38.54	0.14	77.22	−32.96	34.76

[a] Spectra were registered on free iron–porphyrins methanolic solutions and after addition of picpropylen or picdipropylen ligand at 25 °C; δ_H (300 MHz; CD_3OD; $SiMe_4$).

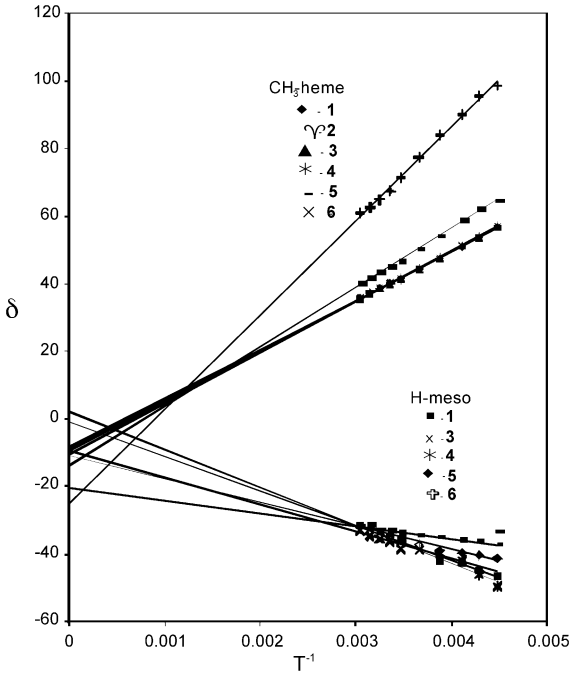

Fig. 4. Curie law plots of $\delta_{\text{heme-CH}_3}$, $\delta_{\text{H-meso}}$, of complexes **1**–**6** vs. T^{-1}. Chemical shifts referenced to $SiMe_4$.

analogous model complexes already reported [31–40]. For **1**–**6,** the *meso* heme proton chemical shifts ($\delta_{\text{H-meso}}$) are between -32 and -36 ppm and the methyl heme proton chemical shifts ($\delta_{\text{CH}_3\text{-heme}}$) are between $\sim$33 and 70 ppm, at RT. The ^{1}H NMR spectra of **1**–**6** were recorded over the temperature range 223–328 K at 10–15 K intervals. Each complex shows both Curie–Weiss and anti-Curie behavior for *meso* and methyl-heme protons, respectively [12,13,31,32,34,36,37] (Fig. 4). The picpropylen axial ligand, common to **1**–**3**, and picdipropylen axial ligand common to **4**–**6**, produce a weak tetragonal field at the porphyrinate-iron(III) site [1–7,9,14,35]. The conditions for the presence of the two types of behavior (Curie–Weiss and anti-Curie) are (1) a contact contribution to the isotropic shifts, and (2) to have unpaired electrons density into a π-symmetry orbital of the ligands [41]. These two conditions, and hence these two behaviors, are not to be realized simultaneously in the same molecule.

H-*meso* signals of **1, 3**–**6** are shifted to lower frequency as the temperature is lowered (anti-Curie behavior). When this relationship is plotted and fitted in a δ vs. $1/T$ graph, its deviation at $T^{-1}\rightarrow 0$ (-20 to $+2$ ppm range) is indicative of a qms state with predominantly $S=\frac{5}{2}$ or $S=\frac{3}{2}$ ground state [2,12–14].

Using the TDF2LVL program [13] the analysis of the temperature dependence of the chemical shifts was carried out with $\frac{W_2}{W_1}=1$, $\frac{6}{4}$ and $\frac{4}{6}$; W_l is the statistical weight of state l. These three weighting ratios represent $S_1=S_2=\frac{3}{2}$, $S_1=\frac{3}{2}$, $S_2=\frac{5}{2}$ and $S_1=\frac{5}{2}$, $S_2=\frac{3}{2}$ [13,41]. The program calculates values for the constants F_1 and F_2. These constants are each simply a combination of the dipolar and contact shifts contributions to the overall chemical shifts of the pyrrol protons for the ground and excited states, at each temperature. Fig. 5 shows the data with a two-level fit for *meso* protons, which is very near to linear dependence. For them F_1 are always negative. These results are in agreement with a nearly empty $d_{x^2-y^2}$ orbital and with electron spin delocalization through π orbitals; for them the $S=\frac{3}{2}$ state is the lowest in energy. Only for **5**, F_2 values are always very small and positive indicating a increase of σ spin delocalization [13]. For the other five new pinch complexes, F_2 takes unexpected negative or zero values, which suggests a null σ delocalization as temperature increases [13] (δ is shifted at lower frequencies). ΔE, the energy separation between the ground state and the first excited state [13], is very small for **1**–**6**, being $S=\frac{3}{2}$ state the lowest in energy.

Forcing a straight line temperature dependence (no $\frac{5}{2}$ spin state) yields the graphs of Fig. 5 with a Curie factor: $F(\mathbf{1})=-10.2\times10^3$, $F(\mathbf{3})=-7.9\times10^3$, $F(\mathbf{4})=-11.2\times10^3$, $F(\mathbf{5})=-6.9\times10^3$, $F(\mathbf{6})=-3.7\times10^3$ ppm K. The latter informs us

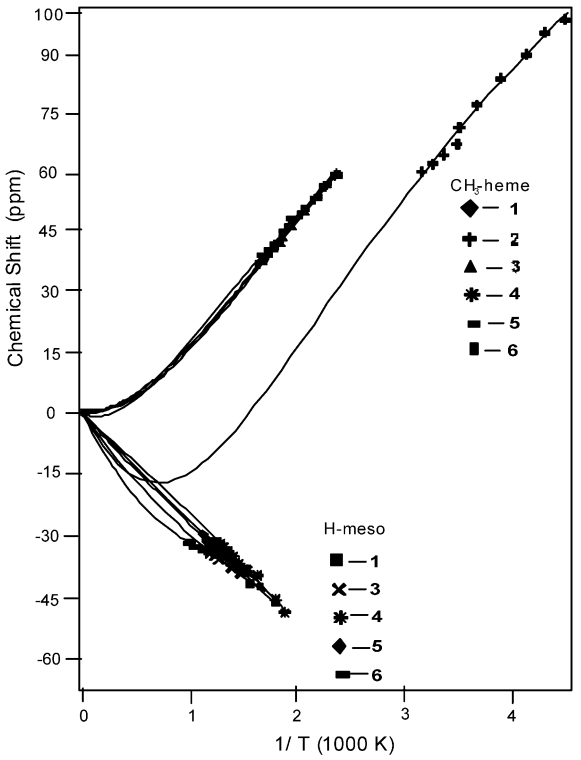

Fig. 5. Isotropic shifts of **1**–**6** of this study as a function of inverse temperature and fits to equation of Shokhirev and Walker [13,39].

that complexes **1**, **3**–**6** have one qms ground state with a high contribution of the $S=\frac{3}{2}$ state, for which the excited qms state with high contribution of the $S=\frac{5}{2}$ state is not thermally accessible.

Behavior of the $CH_{3\text{-heme}}$ chemical shifts of **1**–**6** are more positive as the temperature is lowered, showing a positive slope but a Curie–Weiss behavior in their T^{-1} dependence. At $T^{-1}\rightarrow 0$ the intercept is as large as -8 to -24 ppm. In accord with the methyl heme groups' behavior of **1**–**6** in ^{1}H NMR spectroscopy, their chemical shifts were fitted to the qms two-level dependence on temperature [13]. In all cases F_1 is positive and F_2 negative, and thus qms, ground states with largely $S=\frac{5}{2}$ with $\Delta E > k_B T$ from the qms excited state with largely $S=\frac{3}{2}$ are obtained. Hence, the $d_{x^2-y^2}$ orbital is singly populated allowing σ spin delocalization [13].

The pinch ligands, picpropylen and picdipropylen, have established a weak ligand field which induces some population with qms state largely $S=\frac{3}{2}$ for iron(III) [1,4–9,12,32–42]. These large *ortho*-pyridyl substituted pinch-ligands interact extensively by direct overlap of the electron clouds of the *ortho* substituents and the porphyrin π electrons. The length of the *ortho* chain (seven atoms) of the picpropylen ligand of **1**–**3**, conduces to a weak co-ordination of just one pyridine group, giving rise to the five-co-ordination (Fig. 1). The six-co-ordination site is occupied by a fast interchangeable methanol, water and chloride ligand [13,32–34]. For picdipropylen ligand, the length of the *ortho* chain (11 atoms, Fig. 1) produces a higher steric hindrance, a structure less strained molecule and a six-co-ordination of iron(III), where the two pyridine groups are now co-ordinated.

Both ligands show a fast rotation since the thermal averaging of the two levels is fast on the NMR-time scale.

The magnetic anisotropy in the porphyrin plane, $Q_{\text{asym}}=(\text{spread heme-CH}_3)/(\text{average } \delta_{\text{heme-CH}_3})$, **1**–**3** show values of 0.047–0.067, characteristic of high spin five-co-ordination iron(III) complexes with a small magnetic anisotropy [31]. Mention should be made that Q_{asym} is insensitive to the co-ordination of the solvent and chloride groups [31,32]. It suggests a contact interaction dominating the chemical shifts [31,32] (Table 2). The spread of the four heme-methyl shifts for **1**–**3** reflects differences of the spin delocalization into individual pyrrols with increasing electron withdrawing power of 2,4-*R* porphyrin substituents in the order ethyl < proton ~ vinyl [14,31,32]. The Q_{asym} values of **4**–**6** (0.14–0.18) correspond to six-co-ordinate complexes. The average methyl isotropic shifts do not reflect a net change in iron–porphyrine bonding, which is insensible to the 2,4-*R* peripheral porphyrin substituents [13–15,31].

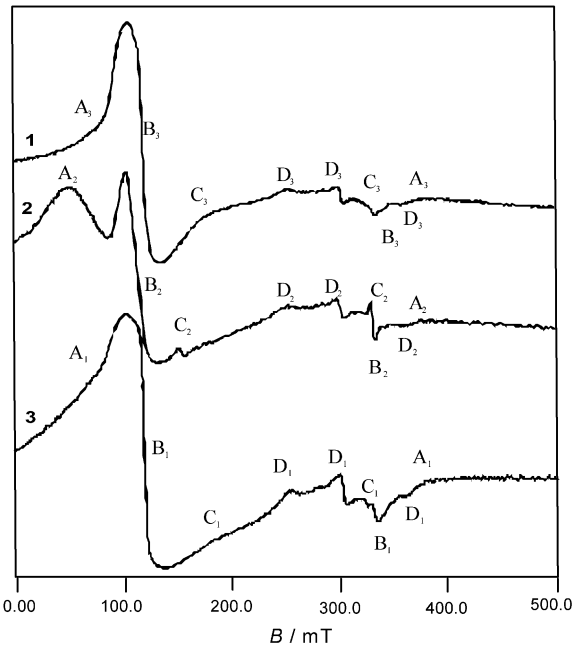

Fig. 6. ESR spectra of complex **1** with the signals A_1,B_1, C_1, D_1; complex **2** with the signals A_2, B_2, C_2, D_2 and complex **3** with the signals A_3, B_3, C_3 and D_3. Experimental parameters: microwave power 1 mW, modulation field of 100 kHz, temperature 77 K.

From these NMR data, it is clear that for all compounds **1**–**6**, there are molecules with the iron(III) in qms ground state, $S=\frac{5}{2}$, $S=\frac{3}{2}$ and other molecules with iron(III) in the other qms ground state $S=\frac{3}{2}$, $S=\frac{5}{2}$. At a given temperature anyone of the compounds **1**–**6** is in a thermal mixture of these two populations.

3.3. ESR spectroscopy

ESR spectra of complexes **1**–**3** are shown in Fig. 6. The presence of several species of iron(III) is observed. These spectra show a signal B at $g_{\perp}^{B}=5.450$ to 5.643 and $g_{\parallel}^{B}\approx 2.0$ (Table 3). This type of signal is common in porphyrin–iron(III) compounds and is assigned to iron(III) paramagnetic species with qms $S=\frac{3}{2}$, $S=\frac{5}{2}$ ground state with largely $S=\frac{5}{2}$ [2–4,13–15,41].

Another species C with $g_{\perp}^{C}\sim 4.20$ to 4.251 ($g_{\parallel}^{C}$ is not observed; low intensity-parallel feature is expected) is observed for **1**–**3** (Table 3). Again, iron(III) paramagnetic species at these $g_{\perp}$ values are assigned to qms $S=\frac{3}{2}$, $S=\frac{5}{2}$ with largely $S=\frac{3}{2}$ [2–4,13–15,40–42]. Another signal D in these three compounds located in the central region is rhombic with $g_x^{D}\sim 2.570$, $g_y^{D}\sim 2.162$ and $g_z^{D}\sim 1.900$ and is assigned to low spin, $S=\frac{1}{2}$, iron(III) paramagnetic species (Table 3) [15].

In addition, the ESR spectra of the three complexes show a very high g value signal, A, at fields lower than 90 mT. Complex **1** and **3** give it at $g\approx 7.95$ and complex **2** gives A at much higher $g\approx 13$. These very high g-value signals are only compatible with porphyrin dimers according to

Table 3
The ESR spectra of **1**–**6** complexes

Complex	Species A	Species B	Species C	Species D
1	$g_{\perp}=7.951$ $g_{\parallel}=1.818$	$g_{\perp}=5.450$ $g_{\parallel}=1.987$	$g_{\perp}=4.200$ $g_{\parallel}\approx 2$	$g_x=2.572$ $g_y=2.158$ $g_z=1.862$
2	$g_{\perp}=13.008$ $g_{\parallel}=1.807$	$g_{\perp}=5.643$ $g_{\parallel}=1.972$	$g_{\perp}=4.231$ $g_{\parallel}\approx 2$	$g_x=2.573$ $g_y=2.157$ $g_z=1.899$
3	$g_{\perp}=7.956$ $g_{\parallel}=1.817$	$g_{\perp}=5.601$ $g_{\parallel}=2.007$	$g_{\perp}=4.251$ $g_{\parallel}\approx 2$	$g_x=2.545$ $g_y=2.162$ $g_z=1.965$
4	$g_{\perp}=7.984$ $g_{\parallel}=1.818$	$g_{\perp}=5.421$ $g_{\parallel}=2.050$	$g_{\perp}=4.200$ $g_{\parallel}\approx 2$	$g_x=2.560$ $g_y=2.154$ $g_z=1.836$
5	$g_{\perp}=12.800$ $g_{\parallel}=1.824$	$g_{\perp}=5.718$ $g_{\parallel}=1.966$	$g_{\perp}=4.279$ $g_{\parallel}\approx 2$	$g_x=2.577$ $g_y=2.148$ $g_z=1.856$
6	$g_{\perp}=7.814$ $g_{\parallel}=1.824$	$g_{\perp}=5.435$ $g_{\parallel}=2.034$	$g_{\perp}=4.279$ $g_{\parallel}\approx 2$	$g_x=2.577$ $g_y=2.148$ $g_z=1.824$

published results (Table 3) [43,44]. Signals A and D are not analyzed in this work since high spin $S=\frac{5}{2}$ and low spin $S=\frac{1}{2}$ compounds have been largely studied [45,46].

ESR spectrum of **4**–**6** are very similar to the spectra of **1–3** (Fig. 6), respectively. Both groups of novel pinch-porphyrins **1–3** and **4–6** show a qms species, B, with largely $S=\frac{5}{2}$ [47] and in high proportion with respect to the other qms species, C, with largely $S=\frac{3}{2}$. In the Maltempo and Moss treatment [3] correlation curves of the crystal splitting (Δ/λ) vs. $g_\perp$ gives for **1**–**6** values of Δ/λ between -1 and -2.17 for the $g_\perp$ values of species B shown in Table 3. The corresponding admixtures of the $\left|\frac{3}{2}\right\rangle$ in the $\left|\frac{5}{2}\right\rangle$ state result in all cases larger than 70% [3,4].

In accord to Nesset et al. [13] for **1**–**6**, it can be said that the iron ion is displaced in the range 0.10–0.30 Å out of the porphyrin plane for $S=\frac{5}{2}$ ground state. Then species B of **1**–**6**, showing qms $\left|\frac{5}{2}\right\rangle$, $\left|\frac{3}{2}\right\rangle$ with largely (70%) $S=\frac{5}{2}$ might have the iron atom displaced out of the plane $\approx$0.30 Å.

For the minority species C in **1**–**6**, again the Maltempo and Moss [3] treatment gives an admixture of $\left|\frac{5}{2}\right\rangle$ into $\left|\frac{3}{2}\right\rangle$ larger than 72.5% and so, for this species it can be said that the iron ion might be displaced out of the plane a distance $\sim$0.10 Å.

Spectroscopic information of the complexes **1**–**3** indicates that they must be hexa-co-ordinated by picpropylen axial ligand and methanol solvent. This is a consequence of the length of the chain with seven atoms [14]. The possibility of a hexa-co-ordination by the picpropylen pinch ligand would produce a very strain structure and a weak co-ordination.

3.4. Peroxidase activity of the complexes 1–6

The catalytic activity of **1**–**6** have confirmed our hypothesis that it is possible to establish a correlation among the population of the $\left|\frac{5}{2}\right\rangle$ state in $\left|\frac{3}{2}\right\rangle$ in qms of iron(III), with the catalytic activity as peroxidase [1,2,12,13,40,41].

The guaiacol (2-methoxyphenol) test is used under conditions for which its oxidation rate with hydrogen peroxide is zero order with respect to its concentration [19].

Eqs. (1)–(3) represent the steady state for the normal horseradish peroxidase with the two intermediate compounds I (HRP-I) and II (HRP-II), the hydrogen donor agent AH_2 and the oxidized products •AH [48].

A ping-pong peroxidase mechanism [48] is utilized and the reaction conditions are similar to those for pinch-porphyrin complexes reported [14].

$$\mathrm{HRP}+\mathrm{H_2O_2}\xrightarrow{k_1}\mathrm{HRP\text{-}I}+\mathrm{H_2O} \quad (1)$$

$$\mathrm{HRP\text{-}I}+\mathrm{AH_2}\xrightarrow{k_2}\mathrm{HRP\text{-}II}+\bullet\mathrm{AH} \quad (2)$$

$$\mathrm{HRP\text{-}II}+\mathrm{AH_2}\xrightarrow{k_3}\mathrm{HRP}+\bullet\mathrm{AH} \quad (3)$$

Eq. (4) is used to analyze the initial rate data of the catalytic activity of **1**–**6** where $[E]_0$=total pinch-porphyrin complex; υ=initial rate, K_A and K_B=Michaelis constants for H_2O_2 and guaiacol; k_{cat}=theoretical maximum rate constant.

$$[E]_0\upsilon^{-1}=K_A\,k_{cat}^{-1}[A]^{-1}+k_{cat}^{-1}(1+K_B[B]^{-1}) \quad (4)$$

Primary plots are obtained with the $[E]_0$ vs. $1/[A]$ graphs as a straight line for each constant and specific concentration of guaiacol [B] (Fig. 7). The secondary plots are obtained from the finite ordinate intercepts of these parallel straight lines vs. $[B]^{-1}$, and they correspond to (Eq. (5)).

$$\text{Primary Intercept (PI)}=(K_B\,k_{cat}^{-1})[B]^{-1}+k_{cat}^{-1} \quad (5)$$

Values of K_B (1/abscissa intercept, finite) and k_{cat}^{-1} (1/ordinate intercept, finite) are calculated by

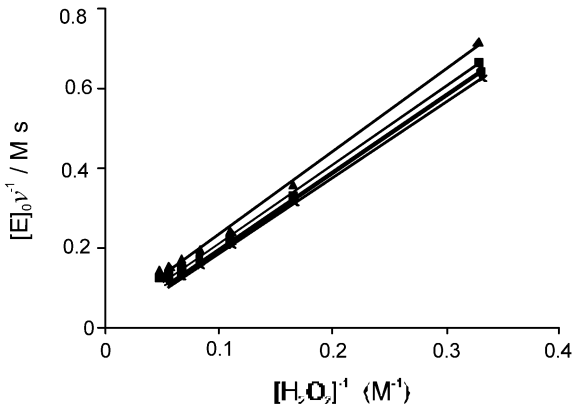

Fig. 7. Plots of ($[E]_0\ v^{-1}$) vs. 1/[A] for compound **4**; $[E]_0$ = 0.020 mM, $[\text{guaiacol}]_f$ = 0.132, 0.198, 0.263 and 0.328 mM, $[H_2O_2]_f$ = 6.07–27.05 mM. Reaction volume was 3 ml; temperature 25 ± 0.01 °C. pH = 8.0.

Eq. (5). Using these last values it is possible to calculate K_A through the slope in Eq. (4) [48].

The initial velocity values are steady state in the final guaiacol concentration of 0.16 mM. When the final peroxide concentration is increased from 2.3 to 27.52 mM the initial rate values also increases for **1**–**6**. In both cases, saturation is observed. When the concentration of pinch-porphyrin **1**–**6** is increased, the initial rate values also rose and saturation is never observed.

The information given by the Michaelis constants of **1**–**3**, **5**, **6** complexes are very similar. The K_A values for **1**–**3**, **5**, **6** indicate a low affinity of each of them for hydrogen peroxide and an even lower affinity of **4**. The K_A values obtained for pinch-porphyrin with picdien ligand already reported [14], show a higher affinity for hydrogen peroxide.

Hence, a higher concentration of hydrogen peroxide is needed in these experiments [48–51]. This indicates that the dissociation constant of the ES complex is equal to K_A if k_6 is much smaller than k_5 and the bond strength of ES complex of **1**–**6** is weaker than for picdien pinch complexes reported ($K_A \sim 10^{-4}$ M) [14,48].

For **1**–**6** the co-ordination of the hydrogen peroxide to the iron(III) is highly difficult.

For **1**–**3** a five-co-ordination is clear, with a sixth position occupied by anyone of the different species present (methanol, chloride, pinch ligands). These species can have a fast exchange in the sixth position. The free rotation of the picpropylen axial ligand in the fifth position produces a steric hindrance for its oxidation by hydrogen peroxide.

For **4**–**6** the pyridine groups occupying two axial sites (five and six) make the co-ordination of the oxidant slow. The same mechanism as for pinch-porphyrins reported is also proposed here for **1**–**6** [14].

The K_B Michaelis constants (respect to guaiacol) are smaller than K_A (at least, by two orders magnitude respect to hydrogen peroxide) as expected (Table 4) [49,50].

The theoretical maximum rate constant, k_{cat}, and the steady state of the pinch-porphyrin **1**–**6** reaction show that guaiacol oxidation is slightly faster than the iron porphyrin autooxidation. However, it is possible that the autooxidation reaction of **1**–**3** complexes could be more frequent by the formation of μ-oxo or μ-peroxo complexes [51–53]. For **4**–**6**, a steric effect of the larger chain would reject the hydrogen peroxide from iron(III) or the guaiacol molecule from iron(IV) (Table 4).

However, **1**–**6** show a low catalytic activity which could be due to the high proportion of the qms B-species which has a high percentage of $S = \frac{5}{2}$ and a low population of the qms C-species with a high percentage of $S = \frac{3}{2}$. It must be noted that this C-species is precisely the one proposed to be responsible for the high peroxidase activity in the previously reported pinch-porphyrins [14].

Table 4
Michaelis and theoretical maximum rate constants experimentally obtained of **1–6**

Complex	K_{H_2O}/M	$K_{guaiacol}$/M	$k_{cat}/M^{-1}s^{-1}$
1	6.6235×10^{-2}	3.388×10^{-4}	9.1074×10^{2}
2	4.5008×10^{-2}	7.67×10^{-5}	4.916×10^{2}
3	4.3096×10^{-2}	5.25×10^{-5}	3.647×10^{2}
4	1.1884×10^{-1}	3.455×10^{-4}	1.0101×10^{3}
5	2.4923×10^{-2}	1.361×10^{-4}	2.701×10^{2}
6	4.1590×10^{-2}	1.170×10^{-4}	3.145×10^{2}

Table S1
Curie factors and energy separations, $k_BT^* > \Delta E$, for two-level fitting of the temperature dependence of the *meso*-protons isotropic shifts of the **1–6** complexes for $W_2/W_1 = 1$

Pinch-porphyrin	δ (ppm) H-meso	10^{-3} F_1 (ppm K)	10^{-3} F_2 (ppm K)	$\lvert\Delta E\rvert$ (cm^{-1})	10^{-3} σ, (ppm K)
1	−38.62	−21.39	0	8.16	0.6
2	–	–	–	–	–
3	−38.55	−27.33	0	88.49	0.6
4	−38.76	−19.01	0	44.60	0.6
5	−37.04	−39.66	13.76	42.51	0.4
6	−34.29	−29.48	−4.65	276.57	0.2

Table S2
Curie factors and energy separations, $k_BT^* > \Delta E$, for two-level fitting of the temperature dependence of the *meso*-protons isotropic shifts of the **1–6** complexes of this study for $W_2/W_1 = 6/4$

Pinch-porphyrin	δ (ppm) H-meso	10^{-3} F_1 (ppm K)	10^{-3} F_2 (ppm K)	$\lvert\Delta E\rvert$ (cm^{-1})	10^{-3} σ (ppm K)
1	−38.62	−8.9	−11.54	68.96	0.6
2	–	–	–	–	–
3	−38.55	−42.80	0	71.62	0.6
4	−38.76	2.47	−15	62.87	0.6
5	−37.04	−49.25	4.09	54.29	0.4
6	−34.29	−46.14	−4.13	230.28	0.2

These new pinch complexes **1**–**6** show that the length of the ligand chain determines the strength and symmetry of the ligand field around iron(III) and in consequence, their electronic and magnetic structures and catalytic activity in the B and C species.

On several natural porphyrins it has been found that the change of the concentration of Ca^{2+} ions at the proximal and distal sites (axial perturbations of the porphyrins structure) plays a critical role in regulating the heme pocket structural and catalytic properties. It has also been reported that the Fe ion spin state is modified by this change and the appearance of a qms spin state is not uncommon [28,54].

Hence, our results on these model pinch porphyrins, are highly consistent with the ones mentioned for natural proteins. Moreover, it should be noted that all class III plant peroxidases described to date, not only horseradish peroxidase, are characterized by a qms heme state [54,55].

For **1**–**3,** the axial ligand is *N*,*N*′-bis-pyridin-2-ylmethyl-propane-1,3-diamine (picpropylen) and is maintained fixed. However, the in-plane porphyrin substitutions are 2,4-CH=CH_2, 2,4-CH_2CH_3 and 2,4-H and for **4**–**6** the axial ligand is *N*-pyridin-2-ylmethyl-*N*′-{3-[(pyridin-2-ylmethyl)-amine]-propyl}-propane-1,3-diamine (picdipropylen) and is also maintained fixed, while the in-plane porphyrin substituents are 2,4-CH=CH_2, 2,4-CH_2CH_3 and 2,4-H, respectively. For all cases **1**–**6,** we found species B and C, which are the ones assigned with the qms spin-state. Hence, it can be concluded that we also observe the appearance of qms by varying or modifying the in-plane heme structure. Recently, Cheng et al. [55] reported complex models of cytochromes *c* and some photosynthetic chromophores with larger ring deformations, saddle-shaped distortions from planarity for the hemes (in-plane perturbations of the structure) as the mechanism that modify the electronic structure and elucidates the appearance of qms spin state in their complexes.

Again, our findings are in agreement with those of Cheng et al. [55] for in-plane perturbations of the heme structure.

Finally, it was possible to establish a correlation among catalytic, structural and magnetic properties of **1**–**6**. The higher the $S = \frac{3}{2}$ spin contribution to the qms ground state and the proportion of this species into the sample, the higher the peroxidase activity. The results of this work give support to our hypothesis that higher percentage of $S = 3/2$ in qms $S = 3/2$, $5/2$ of iron(III) and a higher

Table S3
Curie factors and energy separations, $k_BT^* > \Delta E$, for two-level fitting of the temperature dependence of the *meso*-protons isotropic shifts of the **1–6** complexes of this study for $W_2/W_1 = 4/6$

Pinch-porphyrin	δ (ppm) H-meso	10^{-3} F_1 (ppm K)	10^{-3} F_2 (ppm K)	$\lvert\Delta E\rvert$ (cm^{-1})	10^{-3} σ (ppm K)
1	−38.62	−15.78	0	12.42	0.6
2	–	–	–	–	–
3	−38.55	−19.84	0	117.31	0.6
4	−38.76	−5.39	−18.32	67.26	0.6
5	−37.04	−23.38	9.86	69.34	0.4
6	−34.29	−45.96	51.39	44.61	0.2

Table S4
Curie factors and energy separations, $k_B T^* < \Delta E$, for two-level fitting of the temperature dependence of the methyl-heme isotropic shifts of the **1**–**6** complexes of this study for $W_2/W_1 = 1$

Pinch-porphyrin	δ (ppm) CH_3-heme	10^{-3} F_1 (ppm K)	10^{-3} F_2 (ppm K)	$\lvert\Delta E\rvert$ (cm^{-1})	10^{-3} σ (ppm K)
1	44.44	13.47	−11.84	527.15	0.4
2	77.33	23.37	−132.22	778.60	1.3
3	44.37	13.66	−12.98	514.50	0.4
4	44.39	13.43	−17.20	575.25	0.3
5	45.08	12.58	−21.89	778.60	0.6
6	44.71	13.89	−14.03	499.20	0.4

Table S5
Curie factors and energy separations, $k_B T^* < \Delta E$, for two-level fitting of the temperature dependence of the methyl-heme isotropic shifts of the **1**–**6** complexes of this study for $W_2/W_1 = 6/4$

Pinch-porphyrin	δ (ppm) CH_3-heme	10^{-3} F_1 (ppm K)	10^{-3} F_2 (ppm K)	$\lvert\Delta E\rvert$ (cm^{-1})	10^{-3} σ (ppm K)
1	44.44	13.42	−1.75	570.87	0.4
2	77.33	23.29	−61.89	806.35	1.3
3	44.37	13.59	−2.46	559.15	0.4
4	44.39	13.39	−4.54	614.04	0.3
5	45.08	12.49	−22.23	959.45	0.5
6	44.71	13.81	−3.12	545.40	0.4

Table S6
Curie factors and energy separations, $k_B T^* < \Delta E$, for two-level fitting of the temperature dependence of the methyl-heme isotropic shifts of the **1**–**6** complexes of this study for $W_2/W_1 = 4/6$

Pinch-porphyrin	δ (ppm) CH_3-heme	10^{-3} F_1 (ppm K)	10^{-3} F_2 (ppm K)	$\lvert\Delta E\rvert$ (cm^{-1})	10^{-3} σ (ppm K)
1	44.44	13.52	− 32.43	499.70	0.4
2	77.33	24.08	−136.20	583.80	1.3
3	44.37	13.70	− 34.44	486.32	0.4
4	44.39	13.46	− 43.20	551.58	0.3
5	45.08	12.73	− 21.36	586.80	0.6
6	44.71	13.95	− 36.20	469.81	0.4

proportion of this species determines a higher peroxidase activity.

Appendix A: Supplementary material

Tables S1, S2 and S3 and Tables S4, S5 and S6. Curie factors and energy separations for two-level fitting of the temperature dependence of the *meso*-protons and the methyl-heme protons isotropic shifts of the **1**–**6** complexes for $W_2/W_1 = 1$, $6/4$ and $4/6$.

References

[1] M. Kastner, T. Mashiko, C.A. Reed, Molecular structure of diaquo-α,β,γ,δ-tetraphenylporphyrinatoiron(III) perchlorate and perchlorato-α,β,γ,δ-tetraphenyl-porphyrinatoiron(III). Two new structural types for iron(III) porphyrins, J. Am. Chem. Soc. 100 (1978) 666–667.
[2] C.A. Reed, F. Guiset, A 'magnetochemical series'. Ligand field strengths of weakly binding anions deduced from $S = 3/2$, $5/2$ spin state mixing in iron(III) porphyrins, J. Am. Chem. Soc. 118 (1996) 3281–3286.
[3] M.M. Maltempo, T.H. Moss, M.A. Cusanovich, Magnetic studies on the changes in the iron environment in

chromatium ferricytochrome *c*′, Biochim. Biophys. Acta 342 (1974) 290–305.

[4] M.M. Maltempo, T.H. Moss, The spin 3/2 state and quantum spin mixture in haem proteins, Q. Rev. Biophys. 9 (1976) 181–215.

[5] G. Harris, Spin-mixed states of ferric ion in complexes of tetragonal symmetry, Theor. Chim. Acta (Berl.) 10 (1968) 119–154.

[6] D.R. Evans, C.A. Reed, Reversal of H_2O and OH-ligand field strength on the magnetochemical series relative to the spectrochemical series. Novel 1-equiv water chemistry of iron(III) tetraphenylporphyrin complexes, J. Am. Chem. Soc. 122 (2000) 4460–4467.

[7] H. Ogoshi, H. Sugimoto, Z. Yoshida, ^{1}H NMR and resonance Raman spectra of octaethylporphyrinatoiron(III) perchlorate and its mono imidazole adduct, Biochim. Biophys. Acta 621 (1980) 19–28.

[8] G.P. Gupta 290, G. Lang, Y.J. Lee, R. Scheidt, K. Shelly, C.A. Reed, Spin coupled in admixed intermediate-spin iron(III) porphyrin dimers: crystal structure, mossbauer, and susceptibility study of $Fe(TPP)(B_{11}CH_{12}).C_7H_8$, Inorg. Chem. 26 (1987) 3022–3030.

[9] D.A. Summerville, I.A. Cohen, K. Hatano, W.R. Scheidt, Preparation and physical and stereochemical characterization of the tricyanomethanide salt 5,10,15,20-tetraphenylporphyrintoiron(III). A six-coordinate intermediate-spin complexe, Inorg. Chem. 17 (1978) 2906–2910.

[10] D.H. Dolphin, J.R. Sams, T.B. Tsin, Intermediate-spin ($S=3/2$) porphyrinatoiron(III) complexes, Inorg. Chem. 16 (1977) 711–713.

[11] H. Masuda, T. Taga, K. Osaki, H. Sugimoto, Z. Yoshida, H. Ogoshi, Crystal and molecular structure of (octaethylpotphyrinato)iron(III) perchorate, anomalous magnetic properties and structural aspects, Inorg. Chem. 19 (1980) 950–954.

[12] A.D. Boersma, H.M. Goff, Multinuclear magnetic resonance spectroscopy of spin-admixed $S=3/2$, 5/2 iron(III) porphyrins, Inorg. Chem. 21 (1982) 581–586.

[13] M.J.M. Nesset, S. Cai, T.Kh. Shokhireva, N.V. Shokhirev, S.E. Jacobson, K. Jayaraj, et al., Electronic effects in transition metal prophyrins. 10. Effect of *ortho* substituents on the temperature dependence of the NMR spectra of a series of admixed perchloratoiron(III) tetrakis(2,7- or 2,4,6-phenyl substituted)porphynatos, Inorg. Chem. 39 (2000) 532–540.

[14] Y. Reyes-Ortega, C. Álvarez-Toledano, D. Ramírez-Rosales, A. Sánchez-Sandoval, E. González-Vergara, R. Zamorano-Ulloa, Pinch-porphyrins, new spectroscopic and kinetic models of peroxidases, J. Chem. Soc.; Dalton Trans. (1998) 667–674.

[15] F.A. Walker, Proton NMR and EPR Spectroscopy of Paramagnetic Metalloporphyrins, Academic Press, The Porphyrins Handbook, USA, 1999, pp. 81–175.

[16] J.C.A. Reed, T. Mashiko, S.P. Bentley, M.E. Kastner, W.R. Scheidt, K. Spartalian, et al., The missing heme spin state and a model for cytochrome *c*′. The mixed $S=3/2$, 5/2 intermediate spin ferric porphyrin: perchlorato(*meso*-tetraphenylporphynato)iron(III), J. Am. Chem. Soc. 101 (1979) 2948–2958.

[17] A. Gismelseed, E.L. Bominaar, E. Bill, A.X. Trautwein, H. Winkler, H. Nasri, et al., Six-coordinate quantum-mechanically weakly spin-mixed ($S=3/2$, 5/2) (triflato)aquoiron(III) 'picket-fence' porphyrin complex: synthesis ans structural, Mossbauer, EPR, and magnetic characterization, Inorg. Chem. 29 (1990) 2741–2749.

[18] W.R. Sheidt, S.R. Osvath, Y.J. Lee, C.A. Reed, B. Shaevitz, G.P. Gupta, Control of spin state in iron(III) porphyrinates. The admixed intermediate-spin case. Crystal structure, Mössbauer, and susceptibility study of $[Fe(OEP)(3,5\text{-}Cl_2py)_2]ClO_4$, Inorg. Chem. 28 (1989) 1591–1595.

[19] H.U. Bergmeyer (Ed.), Methods of Enzymatic Analysis, Academic Press, New York, 1974, pp. 494–495.

[20] A.D. Falk, The Porphyrins and Metalloporphyrins, Elsevier, New York, 1964, p. 800.

[21] A. Sánchez-Sandoval, C. Álvarez-Toledano, R. Gutiérrez-Pérez, Y. Reyes-Ortega, A modified procedure for the preparation of linear polyamines, synthetic communications, which will tentatively appear in Vol. 33, Number 3, 2003.

[22] W. Owens, Ch. O'Connor, Comparison of the electronic and vibrational spectra of complexes of protoporphyrin-IX, hemeoctapeptide, and heme proteins, Coord. Chem. Rev. 84 (1988) 1–45.

[23] M. Gouterman, Optical spectra and electronic structure of porphyrins and related rings, in: D. Dolphin (Ed.), The Porphyrins, 3, Academic Press, New York, 1978, pp. 1–69.

[24] M. Zerner, M. Gouterman, H. Kobayashi, Theor. Chim. Acta 6 (1966) 363–400.

[25] E.I. Solomon, M.L. Kirk, D.R. Gamelin, S. Pulver, Bioinorganic spectroscopy, Methods Enzymol. 246 (1995) 71–93.

[26] D. Dolphin, The electronic configurations of catalases and peroxidases in their high oxidation states: a definitive assessment, Isr. J. Chem. 21 (1981) 67–71.

[27] F. Adar, Electronic absortion spectra of hemes and hemeproteins, in: D. Dolphin (Ed.), The Porphyrins, 4, Academic Press, New York, 1978, pp. 167–209.

[28] M.M. Maltempo, P.-I. Ohlsson, K.-G. Paul, L. Petersson, A. Ehrenberg, Electron paramagnetic resonance analyses of horseradish preoxidase in situ and after purification, J. Am. Chem. Soc. 18 (1979) 2935–2940.

[29] A. Boffi, T.K. Das, S. della Longa, C. Spagnuolo, D.L. Rousseau, Pentacoordinate hemin derivatives in sodium dodecyl sulfate micelles, Biophys. J. 77 (1999) 1143–1149.

[30] W.E. Blumberg, J. Peisach, B.A. Wittenberg, J.B. Wittenberg, The electronic structure of protoheme proteins, J. Biol. Chem. 243 (1968) 1854–1862.

[31] D.L. Budd, G.N. La Mar, K.C. Langry, K.M. Smith, N.-R. Mazhir, 1H NMR study of high-spin ferric natural

porphyrin derivatives as models of methemoproteins, J. Am. Chem. Soc. 101 (1979) 6091–6095.
[32] R.J. Kurland, R.G. Little, D.G. Davis, Ch. Ho, Proton magnetic resonance study of high- and low-spin hemin derivatives, Biochemistry 12 (1971) 2237–2246.
[33] J.D. Satterlee, J.E. Erman, Heme asymmetry in deuterohemin-reconstituted cytochrome *c* peroxidase, J. Am. Chem. Soc. 103 (1981) 199–200.
[34] H.A.O. Hill, K.G. Morallee, Nuclear magnetic resonance spectra of bis(pyridinato)iron(III)-protoporphyrin IX complexes, J. Am. Chem. Soc. 94 (1972) 731–738.
[35] G.N. La Mar, D.B. Viscio, K.M. Smith, W.S. Caughey, M.L. Smith, NMR studies of low-spin ferric complexes of natural porphyrin derivatives. 1. Effect of peripheral substituents on the π electronic asymmetry in biscyano complexes, J. Am. Chem. Soc. 100 (1978) 8085–8092.
[36] S. Mazumdar, O.K. Medhi, S. Mitra, Six-coordinated high-spin models for ferric hemoproteins: NMR and ESR study of the diaquo(protoporphyrinato IX)iron(III) cation and aquohydroxo(protoporphyrinato IX)iron(III) intercalated in aqueous detergent micelles, Inorg. Chem. 27 (1988) 2541–2543.
[37] E. González-Vergara, M. Meyer, H.M. Goff, Proton nuclear magnetic resonance spectroscopy of horseradish peroxidase isoenzymes: correlation of distinctive spectra with isoenzyme specific activities, Biochemistry 24 (1985) 6561–6567.
[38] G.N. La Mar, J.T. Jackson, L.B. Dugad, M.A. Cusanovich, R.G. Bartsch, Proton NMR study of the comparative electronic/magnetic properties and dynamics of the acid↔alkaline transition in a series of ferricytochromes *c*′, J. Biol. Chem. 265 (1990) 16 173–16 180.
[39] L.B. Dugad, S. Mitra, Nuclear magnetic resonance of paramagnetic metalloporphyrins, Proc. Indian Acad. Sci. Chem. Sci. 93 (1984) 295–311.
[40] M.M. Maltempo, Magnetic state of an unusual bacterial heme protein, J. Chem. Phys. 61 (1974) 2540–2547.
[41] N.V. Shokhirev, F.A. Walker, Analysis of the temperature dependence of the ^{1}H contact shifts in low-spin Fe(III) model hemes and heme proteins: explanation of 'Curie' and 'anti-Curie' behavior within the same molecule, J. Phys. Chem. 99 (1995) 17 795–17 804.
[42] K. Shelly, T. Bartczak, W.R. Scheidt, C.A. Reed, Coordinated hexafluoroantimonate; X-ray crystal structure of the intermediate-spin iron(III) tetraphenylporphinato complex Fe(TPP)($FSbF_5$)·C_6H_5F, Inorg. Chem. 24 (1985) 4325–4330.
[43] H.G. Jang, M.P. Hendrich, L. Que Jr, Insight into the $g \approx 16$ EPR signals of reduced diiron-oxo proteins. Structure and properties of [Fe^{II}_2BPMP{$O_2P(OC_6H_5)_2$}$_2$]Cl, Inorg. Chem. 32 (1993) 911–918.
[44] B.A. Averill, J.C. Davis, S. Burman, T. Zirino, J. Sanders-Loheer, T.M. Loheer, et al., Spectroscopic and magnetic studies of the purple acid phosphatase from bovine spleen, J. Am. Chem. Soc. 109 (1987) 3760–3767.
[45] N. Nakamura, T. Ikeue, H. Fujii, T. Yoshimura, K. Tajima, Electron configuration and spin distribution in low-spin (*meso*-tetraalkylporphyrinato)iron(III) complexes carrying one or two orientationally fixed imidazole ligands, Inorg. Chem. 37 (1998) 2405–2414.
[46] R.D. Dowsing, J.F. Gibson, Electron spin resonance of high-spin d^5 systems, J. Chem. Phys. 50 (1969) 294–303.
[47] G.S. Lukat, K.R. Rodgers, H.M. Goff, Electron paramagnetic resonance spectroscopy of lactoperoxidase complexes: clarification of hiperfine splitting for the NO adduct of lactoperoxidase, Biochemistry 26 (1987) 6927–6932.
[48] H.B. Dunford, in: J. Everse, K.E. Everse, M.B. Grisham (Eds.), Peroxidases in Chemistry and Biology, 2, CRC Press, Boca Raton, FL, 1990, Chapter 1.
[49] J.T. Groves, Y. Watanabe, Reactive iron porphyrin derivatives related to the catalytic cycles of cytochrome P-450 and peroxidase. Studies of the mechanism of oxygen activation, J. Am. Chem. Soc. 110 (1988) 8443–8452.
[50] T.G. Traylor, W.A. Lee, D.V. Stynes, Model compound studies related to peroxidases. Mechanisms of reactions of hemins with peracids, J. Am. Chem. Soc. 106 (1984) 755–764.
[51] F.S. Woo, M. Cahiwat-Alquiza, H.C. Kelly, Iron porphyrin models of peroxidase enzymes: catalytic activity, regeneration and oxidative degradation of mesoferriheme, Inorg. Chem. 29 (1990) 4330–4718.
[52] A.L. Balch, The reactivity of spectroscopically detected peroxy complexes of iron porphyrins, Inorg. Chim. Acta 198–200 (1992) 297–307.
[53] H.C. Kelly, S.C. Yasui, Iron porphyrin models of peroxidase enzyme intermediates: oxidation of deuteroferriheme by C_6H_5IO and $C_6H_5I(OAc)_2$, Inorg. Chem. 23 (1984) 3559–3563.
[54] B.D. Howes, A. Feis, L. Raimondi, Ch. Indiani, The critical role of the proximal calcium ion in the structural properties of horseradish peroxidase, J. Biol. Chem. 276 (2001) 40 704–40 711.
[55] R.-J. Cheng, P.-Y. Chen, P.-R. Gau, Ch.-Ch. Chen, S.-M. Peng, Control of spin state by ring conformation of iron(III) porphyrins. A novel model for the quantum-mixed intermediate spin state of ferric cytochrome *c*′ from photosynthetic bacteria, J. Am. Chem. Soc. 119 (1997) 2563.